

Response to comments from Anonymous Referee #2

This comment addresses the comments of Anonymous Referee #2. We wish to thank the Referee for the interest in our work and the valuable inputs on the manuscript. The follow document is a point by point response to both the general and specific comments of the Referee.

Note: the following fonts are applied to divide Referee's comments from the Author's response:

Comments from the Referee

Response from the Authors

The page and lines numbers refer to the original version of the manuscript. The manuscript following the Author's response is the final revised version.

General Comments

This manuscript estimated the aerosol indirect effect over the Baltic Sea region by using MODIS L3 dataset. Over high latitude regions, such studies are very limited previously because the available dataset are often unreliable. By making use of twelve years of aerosol and cloud properties from MODIS product, the authors investigated the response of the cloud properties to change of aerosol loading based on statistical analysis, and presented some interesting findings over the region. Overall, this manuscript is well written and useful to improve our understanding on aerosol-cloud interaction. The disadvantage is lacking of the detailed explanations and discussions on the results presented (see my specific comments below).

Each of the specific comments provided by the Referee are addressed below. By discussing the following comments, the Author hopes that the structure of the results and discussion is now better articulated.

Specific comments

P2, Line 26-27: *you raised a question here, but we don't see a clear answer finally.*

The Author finds that the paragraph at page 7, lines 5-11 summarizes the answer to the scientific question introduced in the Introduction section.

Page 4, line 7: The Author changed the verb 'choose' to 'divide'.

P4, line 19-24: *Fig.2: Area 3 AOD is much larger than AI, why?*

Looking at Fig.2, the AI values of Area 3 are denoted by the square marker and color coded in red. These values are higher than the AOD.

P5, line 2-3: *"Indicating the dominance of fine particles, high values of the AE are found over the entire Area 1, ...", Area 1 should be dominated by sea salt, why the fine particles dominate here?*

The Baltic Sea has a peculiar very low salinity. Therefore sea salt aerosols originated by sea spray are not characteristic of Area 1.

P5, line 18-19: *'Over the Norwegian coast the high values of the COT and the CF can be explained by high hygroscopicity of sea spray aerosols, which makes these particles very efficient'. It seems true, but why we don't see the same thing over the coast of Area 1?*

As stated in the previous comment, the Baltic Sea has a peculiar low salinity. Therefore sea salt aerosols originated by sea spray are not characteristic over the Baltic Sea.

P5, line 25: *should be Fig.4e-h.*

Correction accepted. Text changed accordingly.

P5, line 26-27: *Does MODIS provide cloud top height directly?*

The MODIS cloud top height is provided in the cloud product at L2 but not at L3 (the dataset used in this work).

P5, line 32: *why the CF is not affected by aerosol? Any explanations?*

The author misguided the Referee by stating that no aerosols effect was observed on CF in Fig.3. The Author meant that the signal is not very distinct because the CF lines for the aerosol classes are more 'tangled-up' compared to the profiles of the other cloud parameters.

Figure 3 aims, firstly, to answer the question whether aerosols have an impact on cloud vertical development. Results shows that the highest the aerosols, the lowest is the cloud top pressure (hence higher cloud tops). This effect is observable in each cloud parameter (CF, CER, COT, LWP). The effect of aerosols on CF is not missing from Fig.3, as higher aerosol loading leads to higher vertical development, but this is not a result that is directly linked, and observable, in Fig.6 and Fig.7.

Additionally, Fig. 3 also enables the reader to assess the effect of different aerosol loadings on the cloud parameters. While these are clearly visible for CER, COT, LWP, the signal is not as clear and distinct for CF but is not absent either. The CF for the highest AOD (purple line) is dominantly the highest CF value throughout the vertical profile, in accordance with the AIE's theory. This results is also supported in Fig. 6a and Fig. 7 a,g where high aerosol condition corresponds to higher CF.

The text describing the CF results has been modified as following:

Original: " The opposite behavior, lower average values corresponding to the lower classes of the AI/AOD, can be seen for the COT (Fig. 4c, g) and LWP (Figs. 4d, h) while the CF (Fig.4b, f) is not affected by either the AI or AOD."

Rephrased: "The opposite behavior, lower average values corresponding to the lower classes of the AI/AOD, can be seen for the COT (Fig. 4c, g) and LWP (Figs. 4d, h) while the CF (Fig.4b, f) shows a weaker signal for both AI and AOD cases."

P5, line 40-42: *"The cloud droplet size in Area 1 (the Baltic Sea) and Area 2 (Fennoscandia) shows a strong negative correlation with the AI, while a weak correlation is observed over Area 3 (Central-Eastern Europe)", this is contradictory to our understanding.*

Area 3 shows a contradictory results in respect to the AIEs theories.

The effect of saturation of the cloud response to aerosols might be a reason behind the lower negative correlation between CER and AOD. Supporting this theory we note that for low aerosol loadings (AOD, AI < 0.2), a weak negative slope connect CER to AOD over Area 3.

P5, line 42-43: *'Area 1 has no results for the high LWP bins: clouds over the Baltic Sea are most likely stratiform clouds which are characterized by a lower LWP than for convective continental clouds', any references to present that stratiform clouds hold a lower LWP than convective clouds?*

There is a general relationship between cloud type and LWP as shown by Hess et al. (1998), where it was developed a method for deriving atmospheric radiative properties by modelling aerosols and clouds. The cloud model is created by determining classes of different cloud types and their typical microphysical properties. Marine clouds have fewer droplets than continental clouds of the same type. Nonetheless in smaller number, marine cloud droplets are larger: this results in similar LWP in both environments. Stratus and cumulus clouds, in spite of their very different origin, have about the same LWP. Therefore, the reason behind why the clouds over the Baltic Sea (Area 1) have a lower LWP compared to Area 2 and Area 3 is related to the cloud thickness rather than the cloud type.

The author modifies the sentence as following:

Original: "Area 1 has no results for the high LWP bins: clouds over the Baltic Sea are most likely stratiform clouds which are characterized by a lower LWP than for convective continental clouds"

Rephrased: "Area 1 has no results for the high LWP bins. During summer months, few or no convective clouds form over the Baltic Sea, and mainly thin stratiform clouds are identified in the cloud cover."

P5, line 49-p6, line 1: ' ΔCF (Fig. 6a) presents only positive values suggesting that the CF is always significantly larger in the polluted atmospheric conditions'. ΔCF is always negative as I can see. Correction accepted. Text changed accordingly.

P6, line 1-3: '*The positive values of ΔCTP (Fig. 6d) over Area 2 (Fennoscandia) and Area 3 (Central-Eastern Europe) agree with the idea of the vertical development of clouds for higher aerosol loadings (Fig. 4). Higher aerosol loadings cause the vertical development of clouds, and then ΔCTP should be negative, correct?*

If higher aerosol loadings enhance clouds vertical development, ΔCTP is positive because cloud top pressure decreased as a function of altitudes. Therefore, from Eq. 2, $\Delta CTP > 0$.

P6, line 6-8: '*Over land ΔCER is predominantly negative: although small ($< 2 \mu m$), negative values of the ΔCER indicate that the CER is larger over areas with higher aerosol loadings than over cleaner areas. This result is in contradiction with the theory of the AIEs", is there any explanations for this? From Fig. 3, it seems that higher CER correspond to lower aerosol loading, why the contradictory result is shown in Fig. 6?*

Area 3 is the sub-region with overall higher aerosol loadings as we can see from Fig. 2 and Fig. 3. Figure 3 also shows that there is a connection in the spatial distribution between AOD (Fig. 3a) and CER (Fig. 3e) but this represents a qualitative results rather than a physical one.

Aerosol conditions (High-AOD and low-AOD cases) and cloud properties are connected in Figure 6. The result showing negative ΔCER is in contradiction with the first AIE but not necessarily with Fig. 2. As we can see from Fig. 5, the link between CER and AOD for the Central-Eastern Europe has a weak negative slope, from which we formulated the hypothesis of the saturation of the cloud response to an increase of aerosols.

P6, line 15-16: '*The LWP and CER are negatively correlated with aerosol parameters, showing a stronger response to the AOD than to the AI', CER is negatively correlated with aerosol, but LWP is NOT negatively correlated with aerosol from Fig. 7a.*

The author agrees with the Referee. The LWP is increasing as a function of aerosol loading, with a more distinct signal in the AI case (Fig. 7a) than AOD (Fig. 7e). The paragraph is modified accordingly.

P6, line 29-30: '*...0.06 to a maximum of 0.16...*', what is unit? Please keep consistent with the figure. The ACI values for Area 1 are positive, indicating a positive correlation of CER and aerosol loading, right? But why the correlation coefficients are negative?

The values there are related to the ACI, a measure per se that is unit less. The ACI as defined in Eq. 3 has a minus sign in front of the formula. Therefore, ACI values are positive and with a negative correlation.

P6, line 37-38: '*does this result means that high aerosol loading correspond to larger cloud effective radius for Area 3? Can you give some explanations?*

The relationship between CER and AOD is paradoxically positively correlated over Area 3, meaning high aerosol loading correspond to larger cloud effective radius.

One possible explanation might be the indication of the relationship between CTP and AOD: the CTP decreases for increasing AOD (Fig. 4) and at the same time the CER increases with decreasing CTP (higher altitude) in convective clouds (Rosenfeld and Lensky, 1998). Nonetheless, this result must be treated with care as other factors, such as hygroscopic effect, influence the relationship between AOD and cloud parameters and cannot be fully ruled out.

The text above is now included in the manuscript as well as the reference in The Reference section.

References

Hess, M., Koepke, P., and Schult, I.: Optical Properties of Aerosols and Clouds: The Software Package OPAC. *Bull. Amer. Meteor. Soc.*, 79, 831–844, doi: 10.1175/1520-0477(1998)079<0831:OPOAAC>2.0.CO;2, 1998.

Rosenfeld, D., and Lensky, I. M.: Satellite-based insights into precipitation formation processes in continental and maritime convective clouds. *B. Am. Meteorol. Soc.*, 79 (11), 2457-2476, 1998.

1 **Estimates of the aerosol indirect effect over the Baltic Sea region** 2 **derived from twelve years of MODIS observations**

3 Giulia Saponaro¹, Pekka Kolmonen¹, Larisa Sogacheva¹, Edith Rodriguez¹, Timo Virtanen¹ and Gerrit
4 de Leeuw^{1,2}

5 ¹Finnish Meteorological Institute, Helsinki, 00560, Finland

6 ²Department of Physics, University of Helsinki, Helsinki, 00560, Finland

7

8 *Correspondence to:* Giulia Saponaro (giulia.saponaro@fmi.fi) and P. Kolmonen (pekka.kolmonen@fmi.fi)

9 **Abstract.** Twelve years (2003-2014) of aerosol and cloud properties retrieved from the Moderate Resolution Imaging
10 Spectroradiometer (MODIS) on-board the Aqua satellite were used to statistically quantify aerosol-cloud interaction (ACI)
11 over the Baltic Sea region including the relatively clean Fennoscandia and the more polluted Central-Eastern Europe. These
12 areas allowed us to study the effects of different aerosol types and concentrations on macro- and microphysical properties of
13 clouds: cloud effective radius (CER), cloud fraction (CF), cloud optical thickness (COT), cloud liquid water path (LWP) and
14 cloud top height (CTH). Aerosol properties used are aerosol optical depth (AOD), Ångström Exponent (AE) and aerosol index
15 (AI). The study was limited to low level water clouds in the summer.

16 The vertical distributions of the relationships between cloud properties and aerosols show an effect of aerosols on low-level
17 water clouds. CF, COT, LWP and CTH tend to increase with aerosol loading, indicating changes in the cloud structure, while
18 the effective radius of cloud droplets decreases. The ACI is larger at relatively low cloud top levels, between 900 hPa and 700
19 hPa. Most of the studied cloud variables were unaffected by the lower tropospheric stability (LTS) except for the cloud
20 fraction.

21 The spatial distribution of aerosol and cloud parameters and ACI, here defined as the change in CER as a function of aerosol
22 concentration for a fixed LWP, shows positive and statistically significant ACI over the Baltic Sea and Fennoscandia, with
23 the former having the largest values. Small negative ACI values are observed in Central-Eastern Europe, suggesting that large
24 aerosol concentrations saturate the ACI.

25 **Key words:** aerosols, cloud effective radius, aerosol indirect effect, satellite

26 **1 Introduction**

27 Aerosols and especially their effect on the microphysical properties of clouds are among the key components that influence
28 the Earth's climate. As the magnitude and sign of such effects are not well known, understanding and quantifying the influence
29 of aerosols on cloud properties constitute a fundamental step towards understanding the mechanisms of anthropogenic climate
30 change (IPCC, 2013).

31 As aerosols may act as cloud condensation nuclei (CCN), an increase in their number concentration can lead to an increase in
32 the number of cloud droplets in super saturation conditions and a decrease of the cloud droplet radius. The decrease of the
33 droplet effective radius resulting in an increase of the cloud albedo, under the assumption of a constant liquid water path, is
34 known as the Twomey effect (Twomey, 1977). The decrease of droplet size can also impact the precipitation cycle, as the
35 smaller droplets require longer time to grow into precipitating droplet sizes. Additionally, a possible decrease of the
36 precipitation frequency of liquid clouds increases the lifetime of clouds (Albrecht, 1989). These impacts of aerosols are called
37 the first and second indirect effects, respectively.

38 A quantitative evaluation of the effects of aerosols on clouds may be possible mainly in a statistical sense because of the local
39 interactions between meteorological conditions and aerosols (Tao et al., 2012). Satellite-based remote sensing instruments
40 can provide a large data set for statistical analysis from long-term observations of the aerosol indirect effect on a large spatial
41 scale with daily global coverage, complementing localized ground measurements and providing necessary parameters for
42 climate models.

43 A common approach in the satellite-based investigation of the first aerosol indirect effect (AIE) is the concept of the aerosol-
44 cloud-interaction (ACI) that relates the cloud optical thickness (COT), cloud effective radius (CER) or cloud droplet number
45 concentration (CDNC) to the aerosol loading. The aerosol loading is usually expressed by the aerosol optical depth (AOD) or
46 aerosol index (AI, defined in Section 3) that are used as a proxy for the CCN concentration.

47 Many studies describe the interaction between aerosols and clouds through the correlation of the satellite retrieved aerosol
48 concentration and cloud droplet size on a global or regional scale. Inverse correlations on a global (Breon et al., 2002; Myhre
49 et al., 2007; Nakajima et al., 2001) and a regional scale (Costantino et al., 2010; Ou et al., 2013) have been found while
50 Sekiguchi et al. (2003) and Grandey and Stier (2010), applying satellite data on a global scale, found either positive, negative,
51 or negligible correlations between the CER and AOD depending on the location of the observations. Jones et al. (2009)
52 emphasized that the ACI should be inferred in aerosols or cloud regimes determined on a regional-scale, as the relevance of
53 aerosol type, aerosol concentration, and meteorological conditions differ around the world.

54 Areas located at high latitudes are excluded from most of the studies due to a seasonal limitation of the satellite coverage and
55 a smaller number of observations when compared to the global averages over the year. Lihavainen et al. (2010) compared in-
56 situ and satellite measurements to quantify the aerosol indirect effect on low-level clouds over Pallas (Finland), a northern
57 high-latitude site, and concluded that the ACI values derived from ground based measurements were higher than those
58 obtained from satellite observations. Unlike the in situ instruments, the wavelengths used in the satellite retrievals constrain
59 the detection of fine particles to those larger than about 100 nm, thus making it impossible to account for all CCN. Sporre et
60 al. (2014a, 2014b) combined aerosol measurements from two clean, northern high-latitude sites with satellite cloud retrievals
61 and observed that the aerosol number concentration affects the CER while no impact on the COT was observed. As both
62 studies focused on specific locations, no information was thus provided on a larger scale in the Baltic region. This work
63 investigates whether the first indirect effect can be observed also by means of satellite-derived observations over the region
64 of Baltic Sea Countries, a region that offers a northern clean atmospheric background (Fennoscandia) contrasted by a more
65 polluted one (Central-Eastern Europe).

66 Twelve years of aerosol and cloud properties available from the Moderate Resolution Imaging Spectroradiometer (MODIS)
67 retrievals were investigated on a regional scale to determine whether it is possible to observe the response of the properties of
68 low-level liquid clouds to different aerosol loadings in different atmospheric conditions.

69 The satellite retrieval products are introduced in Sect. 2, the approach adopted for the aerosol-cloud interaction analysis is
70 described in Sect. 3, and the results of the analyses are presented in Sect. 4.

71 **2 Data**

72 The area covered in this study is situated at high latitudes (50° N, 10° E, 70° N, 35° E). At these latitudes the solar zenith angle
73 (SZA) constrains the available satellite dataset: a large value of the SZA implies higher uncertainties on the retrieved
74 parameters. Due to the SZA and data coverage constraints, we limit the dataset to summer season (June, July, August)
75 observations that have been collected by the MODIS instrument between 2003 and 2014. Data are analysed only from the
76 MODIS/Aqua platform that crosses the equator at 13:30 local time, when the clouds are fully developed.

77 The MODIS Collection 06 Level 3 (C6 L3) product provides cloud and aerosol parameters at daily time resolution and at a
78 regular 1° x 1° degree spatial grid. The application of MODIS satellite data to aerosol-cloud interaction studies is often
79 criticized for the lack of coincidental aerosol and cloud retrievals. Studies such as Avey et al. (2007), Breon et al. (2002) and
80 Anderson et al. (2003) showed that in the case of daily products at 1° x 1° degree resolution it is unnecessary to individually
81 couple the aerosol and cloud measurements. Therefore, in this study aerosol and cloud data are assumed to be co-located.

82 The MODIS C6 L3 product includes cloud microphysical parameters (CER, COT, LWP) with statistics (mean, minimum,
83 maximum, standard deviation) determined at three different wavelengths (1.6, 2.1 and 3.7 μm) for each cloud phase (liquid,
84 ice, undetermined) separately.

85 We filtered the MODIS cloud data according to the following criteria:

- 86 ▪ Cloud parameters were considered only in the liquid-phase.

- 87 ▪ To eliminate possible outliers, retrievals with a standard deviation higher than the mean values were discarded.
- 88 ▪ Observations with a mean cloud top temperature less than 273 K were eliminated to ensure only warm liquid cloud regimes.
- 89
- 90 ▪ The multi-layer flag was applied to select only single layer clouds.
- 91 ▪ Transparent-cloudy pixels (COT < 5) were discarded to limit uncertainties (Zhang et al., 2012).
- 92 ▪ The CER derived from the 3.7 μm wavelength was chosen as it has been shown to be less affected by the sub-pixel heterogeneity (Zhang et al., 2012).
- 93
- 94 ▪ To exclude precipitating cases, observations were discarded when the difference between CER at 3.7 μm and CER at 2.1 μm was greater than 10 μm (Zhang et al., 2012).
- 95

96 The science data sets (SDS) for the atmospheric aerosol information in the MODIS C6 L3 provides the AOD retrieved at several wavelengths and as a product from the application of either the ‘Deep Blue’ or ‘Dark Target’ algorithm, or a combination of both retrievals (Levy et al., 2013; Sayer et al., 2014). The SDS ‘Aerosol_Optical_Depth_Land_Ocean_Mean’ is the solely product providing the AOD at 0.55 μm globally, while the other aerosol SDSs provide the AOD over land and water separately. As C6 provides the Ångström Exponent (AE) over land only, the AOD at the wavelengths of 0.46 and 0.66 μm present in both ‘Aerosol_Optical_Depth_Land_Mean’ and ‘Aerosol_Optical_Depth_Ocean_Mean’ were used to derive the AE globally as shown in Sect. 3.

103 To assess the effect of meteorological conditions on cloud properties the ECMWF ERA-Interim re-analysis data were applied to derive the Lower Tropospheric Stability (LTS). Although not a ready-to-use product, the LTS is computed as the difference between the potential temperature at 700 hPa and at the surface (Klein and Hartmann, 1993) describing the magnitude of the inversion strength for the lower troposphere.

107 3 Methods

108 After selecting the cloud parameters as listed in the previous section, the number of observations were binned for both aerosol and cloud products. From the obtained histograms, the 95 % of the most frequent ranges were selected from the total dataset by filtering out 2.5 % of data from the extremes. These statistically more robust datasets were used in further analysis.

111 The product of the AOD, representing the column-integrated optical extinction of aerosol at a given wavelength, and the derived AE, describing the spectral dependency of the AOD, results into a third aerosol property of interest, the aerosol index (AI). The AI is used as a proxy for the fine mode aerosol particles which have a larger contribution to the CCN than the coarse mode particles (Nakajima et al., 2001). MODIS Collection 6 provides the AE only over land. To homogeneously estimate the AI over the Baltic Sea and the surrounding land areas, the AE is evaluated by applying equation:

$$116 \quad AE = -\log(AOD_{\lambda_1}/AOD_{\lambda_2})/\log(\lambda_1/\lambda_2), \quad (1)$$

117 to the wavelength pair of $\lambda_1 = 0.66 \mu\text{m}$ and $\lambda_2 = 0.46 \mu\text{m}$ which are available both over land and over sea. The C6 MODIS aerosol algorithm does not, however, allow the determination of the AE for coastal and inland water regions (Levy et al. 2013). This would leave large parts of the Baltic region under investigation in this work out of the analysis (see Fig.3 b and c). For this reason the aerosol-cloud interaction was analysed, in addition to the AI, also with the AOD. Seasonal mean values of aerosol (AOD, AE, AI) and cloud parameters (CER, CF, COT) were computed for the period of 2003-2014.

122 Aiming to observe how the variation in aerosol conditions influences cloud properties, we adopted the approach of Koren et al. (2005) to analyse the average vertical distribution of the relationships between aerosols and cloud properties. The AOD and AI datasets were firstly sorted in ascending order and successively divided into five equally-sampled classes that represent the averages of aerosol conditions for each of the classes. The cloud properties were then divided according to these AI and AOD classes and plotted as functions of cloud top pressure.

127 The response of the cloud properties to clean versus polluted aerosol conditions was studied spatially. The 25th and 75th percentiles of the AI and AOD (AI/AOD) were computed for each spatial grid point, the former constituting the upper limit

129 for the AI/AOD values representing low aerosol loadings and the latter the lower limit for the AI/AOD values for heavy
130 aerosol loadings. These percentile values were then used to divide cloud parameters for clean and polluted aerosol conditions.
131 The difference between a cloud parameter value in low and high aerosol conditions is:

$$132 \quad \Delta\text{Cloud}_X = \text{Cloud}_X_{25\text{th percentile}} - \text{Cloud}_X_{75\text{th percentile}}, \quad (2)$$

133 where the considered cloud parameters, Cloud_X , are the cloud effective radius, cloud top pressure, cloud optical thickness,
134 cloud fraction and liquid water path. The subscripts indicate that the cloud parameter is representative for clean atmospheric
135 conditions, $\text{Cloud}_X_{25\text{th percentile}}$, or for polluted atmospheric conditions, $\text{Cloud}_X_{75\text{th percentile}}$. The difference (ΔCloud_X)
136 between the cloud parameter Cloud_X in clean ($\text{Cloud}_X_{25\text{th percentile}}$) and polluted ($\text{Cloud}_X_{75\text{th percentile}}$) aerosol evidences
137 the impact of these two aerosol cases on the parameter Cloud_X .

138 Matsui et al. (2006) found that aerosols impact the CER stronger in an unstable environment (low LTS) than in a stable
139 environment (high LTS) where the intensity of the ACI is reduced due to the dynamical suppression of the growth of cloud
140 droplets. Following this result, we also compared cloud microphysical properties with both the AI/AOD and the LTS.

141 The area of this study was divided into three sub-regions as presented in Fig. 1: Area 1 covers the Baltic Sea, while Area 2
142 and Area 3 include only land pixels over Fennoscandia and Central-Eastern Europe, respectively. The ACI related to the CER
143 was computed using the formulation from McCominsky and Feingold (2008):

$$144 \quad \text{ACI} = - \left. \frac{\partial \ln \text{CER}}{\partial \ln \alpha} \right|_{\text{LWP}}, \quad (3)$$

145
146 which indicates how a change in the CER depends on a change in the aerosol loading α , given by either the AI or the AOD,
147 for a constant LWP. The ACI was computed by dividing the CER and the AI/AOD over LWP bins ranging from 20 to 300
148 g m^{-2} with an interval of 40 g m^{-2} and then by performing a linear regression analysis with the logarithms of the CER and α
149 in each LWP bin. Two approaches were applied to present the ACI: in the first, the ACI were obtained for each sub-region
150 and plotted as a function of the LWP while in the second approach the ACI was computed in a 2° spatial grid. In the grid
151 approach we chose the LWP interval that provided statistically significant ACI estimates for each of the three sub-regions.
152 The statistical significance is determined by the null-hypothesis test scoring a p-value < 0.05 (Fischer, 1958).

153 **4 Results**

154 Figure 2 presents the time series of AI and AOD averages during the summer months from 2003 to 2014 for each sub-region.
155 It is easy to see in Fig. 2 that these three areas have generally different aerosol conditions: within the land sub-regions, the
156 lower AI and AOD averages occur over Area 2 while over Area 3 these values are higher during the entire period. Area 1, the
157 Baltic Sea, is considered as a third sub-region per se due to the dominance of maritime aerosol conditions. The AI is highest
158 over Area 3 (Central-Eastern Europe), with an overall AI mean value of 0.29 ± 0.03 (regional mean \pm standard deviation),
159 followed by Area 1 (Baltic Sea), 0.20 ± 0.02 , while over Area 2 (Fennoscandia) the lowest AI mean value of 0.16 ± 0.01 is
160 found. Area 3 also presents the highest averages for the AOD, 0.22 ± 0.02 , but Area 2 and Area 1 have comparable AOD
161 values: 0.16 ± 0.02 and 0.14 ± 0.01 , respectively.

162 The spatial variations of the aerosol and cloud properties are shown in Fig. 3. A decreasing south-north gradient of AOD is
163 observed in Fig. 3a where the highest values are found over Area 3 (Northern-Germany and Poland), and the lowest over Area
164 2 (the Atlantic coast of Norway and Northern Sweden). While no discontinuities can be seen for the AOD distribution over
165 Area 1 and Area 2, a clear distinction is evident in the AE (Fig. 3b). Indicating the dominance of fine particles, high values
166 of the AE are found over the entire Area 1, over the Eastern part of Area 3, and over the North-Western part of Area 2. Low
167 values ($\text{AE} < 1$) are only partially found over the land of Areas 2 and 3. The validity of the MODIS AE over land is generally
168 considered unrealistic. Nonetheless, in the case of dominance of fine mode aerosols the MODIS AE agrees with AERONET
169 (Levy et al., 2010) while disagreements occur in coarse aerosol cases (Jethva et al., 2007; Mielonen et al., 2011). Over ocean,
170 a good agreement between MODIS AE and AERONET is found globally with the limitation of $\text{AOD} > 0.2$ (Levy et al., 2015),
171 a restriction that cannot be applied in our study area where the regional AOD is about 0.2. As the sensitivity of AE to AOD
172 errors are especially critical for low AOD values, pixels with $\text{AOD} < 0.2$ are expected to have a less qualitatively accurate AE.

173 Nevertheless, the AE over Area 1 (Fig. 3b) is matching the median range of 1.46-1.49 obtained from a validation study that
174 compares the AE retrieved by SeaWiFS and MODIS Aqua/Terra with the three AERONET stations over the Baltic Sea (Melin
175 et al., 2013). Comparable high AE values are collected by Rodriguez et al. (2012) from 2002 to 2011 at the sub-arctic
176 ALOMAR Observatory (Andøya, Norway): the AE peaks during summer season with a multi-annual mean and standard
177 deviation of 1.3 ± 0.4 . The AI (Fig.3c) over Area 1 is comparable to the values over Area 3, while the lowest values occur
178 over Area 2. The spatial distributions of the cloud properties (COT, CER, CF) are shown in Fig. 3d-f. As in the aerosol case,
179 Area 2 presents a distinctive discontinuity between land and water pixels (Fig3 d-f). These results are confirmed in Karlsson
180 (2003) where Area 1 (the Baltic Sea) exhibits low cloudiness while high cloud amounts are found over the Scandinavian
181 mountain range (Area 2) and the Norwegian Sea. Considering the theory of the first AIE, that is, an increase in aerosol loading
182 leads to larger CDNC and smaller CER for a fixed LWP, the CER (Fig. 3e) shows correlation with the AOD spatial distribution
183 (Fig. 3a) while worst comparison are found between CER (Fig.3e) and AI (Fig.3c). Over the Norwegian coast the high values
184 of the COT, CER and the CF can be explained by high hygroscopicity of sea spray aerosols, which makes these CCN particles
185 very efficient. Another feature of Fig. 3e is the low effective droplet radius over Area 1 (the Baltic Sea). Unlike Area 3
186 (Central-Eastern Europe), Area 1 does not match with any high aerosol loading (Fig. 3a, c) when compared to the surrounding
187 area. In fact, the AOD over Area 1 is as low as in Area 2 (Fig. 2), even though for these land areas the CER is about 1-2 μm
188 larger.

189 Figure 4 presents the 10-year average of the cloud properties, divided into five classes of the AI (Fig. 4a-d) and AOD (Fig.
190 4e-h), respectively, plotted as function of cloud top pressure. It can be observed that the lowest values of CTP correspond to
191 the higher classes of AI/AOD. Assuming the CTP to be an indicator of the cloud top height, this may suggest an enhancement
192 of the cloud vertical structure. This result was also found by Koren et al. (2005) where convective clouds over the North
193 Atlantic showed a strong correlation between the aerosol loading and the vertical development of the clouds. Furthermore,
194 the cloud droplet effective radius (Fig. 4a, e) has smaller values in higher AI/AOD classes. The opposite behaviour, lower
195 average values corresponding to the lower classes of the AI/AOD, can be seen for the COT (Fig. 4c, g) and LWP (Figs. 4d,
196 h) while the CF (Fig.4b, f) shows a weaker signal for both AI and AOD cases. Overall, Fig. 4 reveals that the cloud parameters
197 are clearly affected by the AI/AOD segregation at lower levels of CTP. For this reason, we limit our dataset to cloudy pixels
198 where the CTP is between 700 hPa and 900 hPa.

199 In Fig. 5 the CER is plotted as a function of AI for fixed values of the LWP (five intervals as above) and the CTP (between
200 700 and 950 hPa, in 50 hPa bins). The highest AI in Area 1 (the Baltic Sea) is around 0.35 for the lowest clouds (CTP 900-
201 950 hPa) decreasing to 0.3 for the highest clouds (CTP 700-750 hPa). Over Area 2 (Fennoscandia) the aerosol loading is not
202 clearly connected to the cloud height, showing a constant AI average of approximately 0.25. As expected, Area 3 has the
203 highest average of AI out of the three sub-regions with values as high as 0.6 for the lowest clouds and a small decrement for
204 the highest clouds. The cloud droplet size in Area 1 (the Baltic Sea) and Area 2 (Fennoscandia) shows a strong negative
205 correlation with the AI, while a weak correlation is observed over Area 3 (Central-Eastern Europe). Area 1 has no results for
206 the high LWP bins: during summer months few or no convective clouds form over the Baltic Sea and mainly thin stratiform
207 clouds are identified in the cloud cover. Similar results are also found when the AOD is substituted by the AI (not shown).

208 Applying Eq. 2 to the cloud parameters, the impact of low and high aerosol loading (ΔCloud_X) on cloud properties
209 (Cloud_X) is presented in Fig. 6. Resulting from a grid-based analysis, $\Delta\text{Cloud}_X < 0$ means that the observed cloud parameter,
210 Cloud_X , has a larger value in polluted cases (AI/AOD > 75th percentile) than in clean atmospheric conditions (AI/AOD <
211 25th percentile) for that grid cell and vice versa, when ΔCloud_X has a positive value. As similar results were obtained by
212 applying the AOD and AI, only the results for the AOD are shown. ΔCF (Fig. 6a) presents only negative values suggesting
213 that the CF is always significantly larger in the polluted atmospheric conditions. The positive values of ΔCTP (Fig. 6d) over
214 Area 2 (Fennoscandia) and Area 3 (Central-Eastern Europe) agree with the idea of the vertical development of clouds for
215 higher aerosol loadings (Fig. 4) but other factors, such as surface heating, might be also contributing to the results: the presence
216 of stronger turbulence over land cause the clouds to rise higher than in the presence of lower turbulence, for example, over a
217 cooler water surface. The CER (Fig. 6c) shows a different behaviour over land (Area 3) than over water (Area 1). Over Area
218 3 ΔCER is predominantly negative: although small (< 2 μm), negative values of the ΔCER indicate that the CER is larger
219 over areas with higher aerosol loadings than over cleaner areas. This result is in contradiction with the theory of the AIEs.
220 The presence of aerosol appears to have little or no effect on ΔCOT (Fig. 6b) and ΔLWP (Fig. 6e).

221 In an attempt to connect the link between aerosol and cloud with meteorology, we evaluated the variability of low-level liquid
222 cloud properties as function of aerosol conditions (AOD/AI) and lower troposphere stability (LTS). Figure 7 shows the cloud
223 properties (LWP, CER, CF and COT) plotted as a function of the LTS and AI/AOD. While the CF shows a gradient for both
224 direction of the LTS and the AI/AOD, the other cloud variables (LWP, CER, COT) are mainly affected by aerosols with little
225 to no correlation to changes in the LTS. Higher aerosol values correspond to a smaller CER (Fig.7 b,f) and higher CF (Fig. 7
226 c,g) and LWP (fig. 7a), in agreement with the AIEs, except for the LWP (Fig. 7e) that decreases as a function of the AOD.
227 The LWP (Fig. 7e) shows a non-monotonic response by increasing when the AOD ranges between 0.3-0.4, because at high
228 aerosol concentrations the cloud droplets are smaller and less likely to precipitate, and further the LWP slightly decreases. A
229 possible explanation of a better correlation of the LWP with the AI than with AOD might be found by looking at the LWP
230 vertical distributions in Fig. 4 that indicate a more distinctive separation of the LWP for the AI-based classes than for AOD.

231 Figure 8 illustrates the ACI estimate for the CER (Fig. 8a) and its corresponding correlation coefficient r (Fig. 8b) calculated
232 for the three sub-regions as a function of the LWP bins for both AOD and AI. The lines are color-coded according to the three
233 areas as defined in Fig. 1. The ACI estimates for Area 1 (Baltic Sea) are positive and statistically significant for most of the
234 LWP range increasing, as a function of LWP, from a minimum of 0.06 to a maximum of 0.16 and with a corresponding r
235 ranging from -0.1 to -0.53. The values of the ACI for Area 2 range between 0.02 - 0.06 with fewer statistically significant
236 points and a smaller r than in Area 1. The results collected over both Area 1 and Area 2 appear to be little effected by whether
237 the AOD or AI is applied in the computation of the ACI. For Area 3 two points of the ACI results are statistically significant
238 but with very low values for correlations ($r < 0.1$) for the first two bins of the LWP and, unlike the other two sub-regions, they
239 show a negative sign. The ACI values are statistically significant for the three sub-regions for the first two bins of LWP and
240 when the AOD is chosen over the AI as α . With a combination of these requirements, we derived the spatial distribution of
241 the ACI and r which are shown in Fig. 9. Positive correlations are found predominantly over Area 3, and scattered over Area
242 2, while negative values are covering the majority of Area 1 and, more sparsely, Area 2. The relationship between CER and
243 AOD is, paradoxically, positively correlated over Area 3 suggesting that high aerosol loading correspond to larger cloud
244 effective radius. One possible explanation might be the indication of the relationship between CTP and AOD: the CTP
245 decreases for increasing AOD (Fig.4) and at the same time the CER increases with decreasing CTP (higher altitude) in
246 convective clouds (Rosenfeld and Lensky, 1998). Nonetheless, this result must be treated with care as other factors, such as
247 hygroscopic effect, influence the relationship between AOD and cloud parameters and cannot be fully ignored.

248 5 Discussion and Conclusions

249 In this work we have studied the applicability of satellite-based information for quantifying the aerosol-cloud interaction over
250 the Baltic Sea region. Distinct sub-regional differences were found in the estimates of the ACI related to the effective radius
251 of cloud droplets. No clear ACI results were observed for the other cloud parameters which suggest that these may be
252 influenced by other factors, such as the local meteorological conditions. The meteorological conditions are represented here
253 by the LTS which was compared to the cloud parameters. The LTS is correlated with the CF while no effect was observed
254 upon the other cloud parameters. In particular, there is no clear evidence of the effect of LTS on the interaction between
255 aerosols and cloud effective radius.

256 One of the key aspects of this study was to find out whether a rigorously filtered Level 3 MODIS dataset can be applied for
257 aerosol-cloud interaction studies at a regional level. As the northerly location of the region of interest here restrains the
258 availability of the MODIS observations to the summer months (JJA), one of the challenges is the limited data coverage.
259 Moreover, the selection of specific cloud regimes and the co-location of aerosol and cloud observations are additional essential
260 key factors in building-up a robust dataset which however further decreases the amount of data-points available. As far as
261 known to the authors, no previous results on ACI from a satellite perspective are provided over this area.

262 This study shows that the different aerosol conditions characterizing the Baltic Sea countries have an impact on the ACI and
263 this can be also observed on a regional scale. According to ACI theory, polluted atmospheric conditions are connected with
264 clouds characterized by lower cloud top pressure, larger coverage and optical thickness. However, the cloud effective radius
265 strictly follows the AIE's theory only over Area 1 (the Baltic Sea) which agrees also with the results presented by Feingold
266 (1997). As reported in this study, the CER retrieved in clean clouds is mainly affected by the LWP and aerosol presence while
267 when detected under polluted conditions it additionally shows a high dependence on other factors.

268 The cleaner atmosphere characterizing Area 1 (the Baltic Sea) and Area 2 (Fennoscandia) reveals statistically significant and
269 positive ACI estimates between the CER and AOD that are in agreement with the values obtained from ground-based
270 measurements collected at the sites of Pallas and Hyytiälä in Finland, and Vavihill in Sweden (Lihavainen et al., 2010; Sporre
271 et al., 2014b) while over the more polluted Area 3 (Central-Eastern Europe) the sensitivity to determine the ACI locally is
272 smaller. It can be assumed that more aerosols leads to a high concentration of the CCNs and this lowers the average droplet
273 radius as can be seen in Fig. 3e when the radius is compared between areas located South (high aerosol load) and North (low
274 aerosol load) of the Baltic Sea.

275 Our analysis of the ACI for the CER shown in Fig. 8 leads to the following conclusions:

- 276 • The lowest values of the ACI can be seen over Area 3. This is also the sub-region with the highest average AOD
277 values leading to the smallest cloud droplet size. A further addition of aerosol particles and thus possibly also CCNs
278 does not decrease the cloud droplet size any further. Most of the ACI values are actually negative but very close to
279 zero.
- 280 • The positive ACI values for Area 2 shows that the addition of aerosols to a relatively clean atmosphere does decrease
281 the droplet size.
- 282 • The AI over the land areas in the study should be considered unrealistic because the average inland AE can have
283 values below 1.
- 284 • The average AE over Area 1 has values as high as 1.4 to 1.5. These values, however, can be trusted and have been
285 evaluated by Melin et al. (2013).
- 286 • The low CER over Area 1 requires further explanation. The most probable cause for the low values, based on the
287 MODIS cloud retrieval, is the relatively low cloud top height over the sea. As cloud droplets generally grow in size
288 from the cloud base towards the cloud top (McFiggans et al., 2006), Fig. 4 confirms that the average CER increases
289 with the decreasing CTP. Furthermore, in Fig. 5 there is a distinctive lack of results for high LWP values indicating
290 that there are fewer clouds at higher top heights. These reasons altogether lead to low values of the CER over Area
291 1 as the MODIS instrument retrieves the droplet radius at cloud top, and the top height CER results are low when
292 compared to the surrounding over-land values.
- 293 • The ACI over Area 1 has considerably higher values than over the land sub-regions, and there is a difference in the
294 magnitude between the ACI values determined using the AOD or AI. The clean maritime atmospheric conditions
295 lead to the high sensitivity of droplet size to changes in fine particle concentrations. The AOD and AI difference in
296 ACI, the latter being the higher, indicates that the ACI is caused by fine particles as expected.

297 Another way to assess the aerosol induced changes in cloud parameters would be to analyse time series to find out whether
298 dynamically decreasing or increasing aerosol loading has an effect on clouds. This sort of approach was not attempted in this
299 work.

300 Another important result of this work is the comparison of the ACIs obtained using the AI and AOD, chosen as proxies for
301 the CCN, in order to determine which option leads to more realistic results. Even though theoretically the AI would be a better
302 parameter than AOD to indicate the presence of fine mode aerosol particles, the impact of uncertainties of the derived AI
303 might be substantial.

304 **Data availability**

305 All data used in this study are publicly available. The satellite data from the MODIS instrument used in this study were
306 obtained from <http://ladsweb.nascom.nasa.gov/index.html>. The ECMWF ERA-Interim data were collected from the ECMWF
307 data server http://apps.ecmwf.int/dataset/data/interim_full_daily/.

308 **Acknowledgements**

309 This research was funded by the Maj and Tor Nessling Foundation (grant no. 201600287). The authors also acknowledge
310 the Academy of Finland Centre of Excellence (grant no. 272041).

311 **References**

- 312 Albrecht, B. A: Aerosols, cloud microphysics, and fractional cloudiness. *Science*, 245, 1227-1230, 1989.
- 313 Anderson, T. L., Charlson, R. J., Winker, D. M., Ogren, J. A., and Holmen, K.: Mesoscale variations of tropospheric aerosols.
314 *J. Atmos. Sci.*, 60, 119-136, doi: 10.1175/1520-0469(2003)060<0119:MVOTA>2.0.CO;2, 2003.
- 315 Avey, L., Garrett, T. J., and Stohl, A.: Evaluation of the aerosol indirect effect using satellite, tracer transport model, and
316 aircraft data from the International Consortium for Atmospheric Research on Transport and Transformation. *J. Geophys.*
317 *Res.*, 112, 2156-2202, doi: 10.1029/2006JD007581, 2007.
- 318 Bréon, F.-M., Tanré, D., and Generoso, S.: Aerosol effect on cloud droplet size monitored by satellite. *Science*, 295, 834-
319 838, L11801, doi: 10.1126/science.1066434, 2002.
- 320 Costantino, L., and Bréon, F.-M.: Analysis of aerosol-cloud interaction from multi-sensor satellite observations. *Geophys.*
321 *Res. Lett.*, 37, doi: 10.1029/2009GL041828, 2010.
- 322 Feingold, G.: Modeling of the first indirect effect: Analysis of measurements requirements. *Geophys. Res. Lett.*, 30, 1-4.
323 doi: 10.1029/2003GL017967, 1997.
- 324 Fisher, R.: *Statistical methods for research workers*. Hafner, New York, 1958.
- 325 Grandey, B. S. and Stier, P.: A critical look at spatial scale choices in satellite-based aerosol indirect effect studies. *Atmos.*
326 *Chem. Phys.*, 10, 11459-11470, doi: 10.5194/acp-10-11459-2010, 2010.
- 327 Jethva, H., Satheesh, S. K., and Srinivasan, J.: Assessment of second-generation MODIS aerosol retrieval (Collection 005) at
328 Kanpur, India. *Geophys. Res. Lett.*, 34, 1944-8007, doi:10.1029/2007GL029647, 2007
- 329 Jones, T. A., Christopher, S. A., and Quaas, J.: A six year satellite-based assessment of the regional variations in aerosol
330 indirect effects. *Atmos. Chem. Phys.*, 9, doi: 4091-4114, 10.5194/acp-9-4091-2009, 2009.
- 331 Karlsson, K.-G. (2003). A 10 year cloud climatology over scandinavia derived from NOAA advanced very high resolution
332 radiometer imagery. *Int. J. Climatol.*, 23, 1023-1044, doi: 10.1002/joc.916, 2003.
- 333 Klein, S. A., and Hartmann, D. L.: The seasonal cycle of low stratiform clouds. *J. Climate*, 6, 1587–1606, doi: 10.1175/1520-
334 0442(1993)006<1587:TSCOLS>2.0.CO;2, 1993.
- 335 Koren, I., Kaufman, Y. J., Rosenfeld, D., Remer, L. A., and Rudich, Y.: Aerosol invigoration and restructuring of Atlantic
336 convective clouds. *Geophys. Res. Lett.*, 32, L14828, doi: 10.1029/2005GL023187, 2005.
- 337 Levy, R. C., Remer, L. A., Kleidman, R. G., Mattoo, S., Ichoku, C., Kahn, R., and Eck, T. F. : Global evaluation of the Collection
338 5 MODIS dark-target aerosol products over land. *Atmos. Chem. Phys.*, 10, 10399-10420, doi: 10.5194/acp-10-10399-2010,
339 2010.

340 Levy, R. C., Mattoo, S., Munchak, L. A., Remer, L. A., Sayer, A. M., Patadia, F., and Hsu, N. C.: The Collection 6 MODIS
341 aerosol products over land and ocean. *Atmos. Meas. Tech.*, 6, 2989-3034, doi: 10.5194/amt-6-2989-2013, 10.5194/amt-6-
342 2989-2013, 2013.

343 Levy, R. C., Munchak, L. A., Mattoo, S., Patadia, F., Remer, L. A., and Holz, R. E.: Towards a long-term global aerosol optical
344 depth record: applying a consistent aerosol retrieval algorithm to MODIS and VIIRS-observed reflectance. *Atmos. Meas.*
345 *Tech.*, 8, 4083-4110, doi: 10.5194/amt-8-4083-2015, 2015.

346 Lihavainen, H., Kerminen, V.-M., and Remer, L. A.: Aerosol-cloud interaction determined by both in situ and satellite data
347 over a northern high-latitude site. *Atmos. Chem. Phys.*, 10, 10987-10995, doi: 10.5194/acp-10-10987-2010, 2010.

348 Matsui, T., Masunaga, H., Kreidenweis, S. M., Pielke, R. A., Tao, W.-K., Chin, M., and Kaufman, Y. J.: Satellite-based
349 assessment of marine low cloud variability associated with aerosol, atmospheric stability, and diurnal cycle. *J. Geophys.*
350 *Res.*, 111, D17204, doi: 10.1029/2005JD006097, 2006.

351 McCominsky, A., and Feingold, G.: Quantifying error in the radiative forcing of the first aerosol effect. *Geophys. Res. Lett.*,
352 35, L02810, doi: 10.1029/2007GL032667, 2008.

353 McFiggans, G., Artaxo, P., Baltensperger, U., Coe, H., Facchini, M. C., Feingold, G., Fuzzi, S., Gysel, M., Laaksonen, A.,
354 Lohmann, U., Mentel, T. F., Murphy, D. M., O'Dowd, C.D., Snider, J. R., and Weingartner, E.: The effect of physical and
355 chemical aerosol properties on warm cloud droplet activation. *Atmos. Chem. Phys.*, 6, 2593-2649, doi: 10.5194/acp-6-
356 2593-2006, 2006.

357 Melin, F., Zibordi, G., Carlund, T., Holben, B., and Stefan, S.: Validation of SeaWiFS and MODIS Aqua/Terra aerosol
358 products in coastal regions of European marginal seas. *Oceanologia*, 55, 27-51, doi: 10.5697/oc.55-1.027, 2013.

359 Mielonen, T., Levy, R. C., Aaltonen, V., Komppula, M., de Leeuw, G., Huttunen, J., Lihavainen, H., Kolmonen, P., Lehtinen, K.
360 E. J., and Arola, A.: Evaluating the assumptions of surface reflectance and aerosol type selection within the MODIS aerosol
361 retrieval over land: the problem of dust type selection. *Atmos. Meas. Tech.*, 4, 201-214, doi: 10.5194/amt-4-201-2011,
362 2011.

363 Myhre, G., Stordal, F., Johnsrud, M., Kaufman, Y. J., Rosenfeld, D., Storelvmo, T., Kristjansson, J. E., Berntsen, T. K., Myhre,
364 A., and Isaksen, I. S. A.: Aerosol-cloud interaction inferred from MODIS satellite data and global aerosol models. *Atmos.*
365 *Chem. Phys.*, 7, 3081-3101, doi: 10.5194/acp-7-3081-2007, 2007.

366 Nakajima, T., Higurashi, A., Kawamoto, K., and Penner, J. E.: A possible correlation between satellite-derived cloud and
367 aerosol microphysical parameters. *Geophys. Res. Lett.*, 28, 1171-1174, 2001.

368 Ou, S., Liou, K., Hsu, N., and Tsay, S.: Satellite remote sensing of dust aerosol indirect effects on cloud formation over
369 Eastern Asia. *Int. J. Remote Sens.*, 33, 7257-7272, doi: 10.1080/01431161.2012.700135, 2013.

370 Rodriguez, E., Toledano, C., Cachorro, V. E., Ortiz, P., Stebel, K., Berjón, A., Blindheim, S., Gausa, M. and de Frutos, A.
371 M.: Aerosol characterization at the sub-arctic site Andenes (69°N, 16°E), by the analysis of columnar optical properties.
372 *Q.J.R. Meteorol. Soc.*, 138, 471-482, doi:10.1002/qj.921, 2012.

373 Rosenfeld, D., and Lensky, I. M.: Satellite-based insights into precipitation formation processes in continental and maritime
374 convective clouds. *B. Am. Meteorol. Soc.*, 79 (11), 2457-2476, 1998.

375 Sayer, A. M., Munchak, L. A., Hsu, N. C., Levy, R. C., Bettenhausen, C., and Jeong, M.-J.: MODIS Collection 6 aerosol
376 products: Comparison between Aqua's e-Deep Blue, Dark Target, and "merged" data sets, and usage recommendations. *J.*
377 *Geophys. Res.- Atmos.*, 119, 13.965-13.989, doi: 10.1002/2014JD022453, 2014.

378 Sekiguchi, M., Nakajima, T., Suzuki, K., Kawamoto, K., Higurashi, A., Rosenfeld, D., Sano, I., and Mukai, S.: A study of the
379 direct and indirect effects of aerosols using global satellite data sets of aerosols and cloud parameters. *J. Geophys. Res.-*
380 *Atmos.*, 108, 4699, doi: 10.1029/2002JD003359, 2003.

381 Sporre, M. K., Swietlicki, E., Glantz, P., and Kulmala, M.: A long-term satellite study of aerosol effects on convective clouds
 382 in Nordic background air. *Atmos. Chem. Phys.*, 14, 2203-2217, doi: 10.5194/acp-14-2203-2014, 2014a.

383 Sporre, M. K., Swietlicki, E., Glantz, P., and Kulmala, M.: Aerosol indirect effects on continental low-level clouds over
 384 Sweden and Finland. *Atmos. Chem. Phys.*, 14, 12167-12179, doi: 10.5194/acp-14-12167-2014, 2014b.

385 Stocker, T., Qin, D., Plattner, G.-K., Alexander, L., Allen, S., Bindoff, N., Bréon, F.-M., Church, J.A., Cubasch, U., Emori, S.,
 386 Forster, P., Friedlingstein, P., Gillett, N., Gregory, J. M., Hartmann, D. L., Jansen, E., Kirtman, B., Knutti, R., Krishna Kumar,
 387 K., Lemke, P., Marotzke, J., Masson-Delmotte, V., Meehl, G. A., Mokhov, I. I., Piao, S., Ramaswamy, V., Randall, D., Rhein,
 388 M., Rojas, M., Sabine, C., Shindell, D., Talley, L. D., Vaughan, D. G., and Xie, S.-P.: Technical Summary. In *Climate Change*
 389 *2013: The Physical Science Basis. Contribution of Working Group I to the Fifth Assessment Report of the*
 390 *Intergovernmental Panel on Climate Change*, 1535, Cambridge, United Kingdom and New York, NY, USA: Cambridge
 391 University Press, doi:10.1017/CBO9781107415324, 2013.

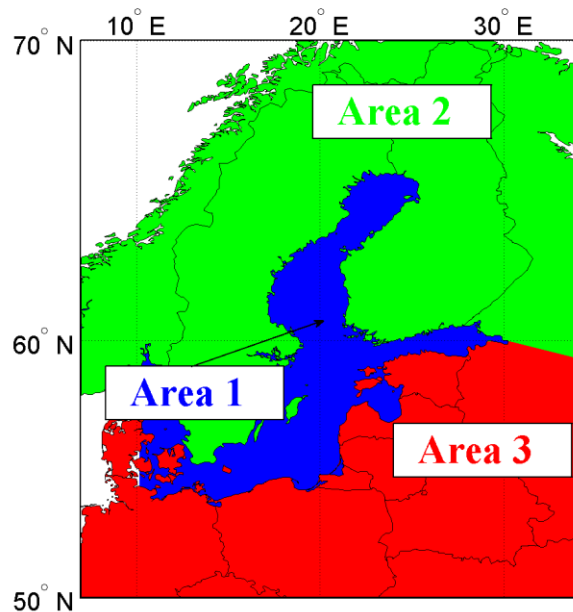
392 Tao, W.-K., Chen, J.-P., Zhanqing, L., Wang, C., and Zhang, C.: Impact of aerosols on convective clouds and precipitation.
 393 *Rev. Geophys*, 50, RG2001, doi: 10.1029/2011RG000369, 2012.

394 Twomey, S.: Influence of pollution on the short-wave albedo of clouds. *J. Atmos. Sci*, 34, 1149-1152, 1977.

395 Zhang, Z., Ackerman, A. S., Feingold, G., Platnick, S., Pincus, R., and Xue, H.: Effects of cloud horizontal inhomogeneity and
 396 drizzle on remote sensing of cloud droplet effective radius: Case studies based on large-eddy simulations. *J. Geophys. Res.*,
 397 117, D19208, doi: 10.1029/2012JD017655, 2012.

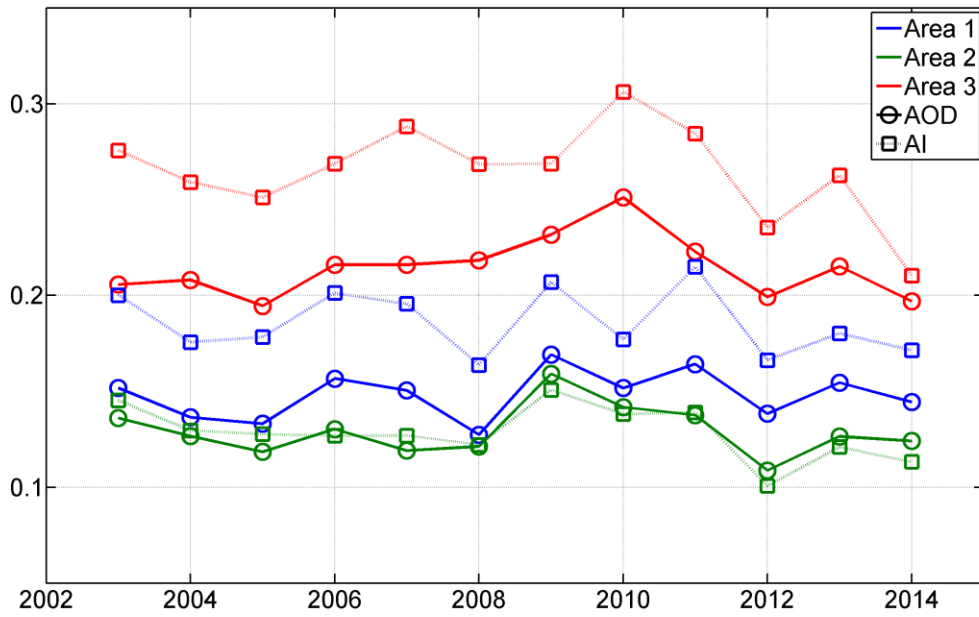
398

399



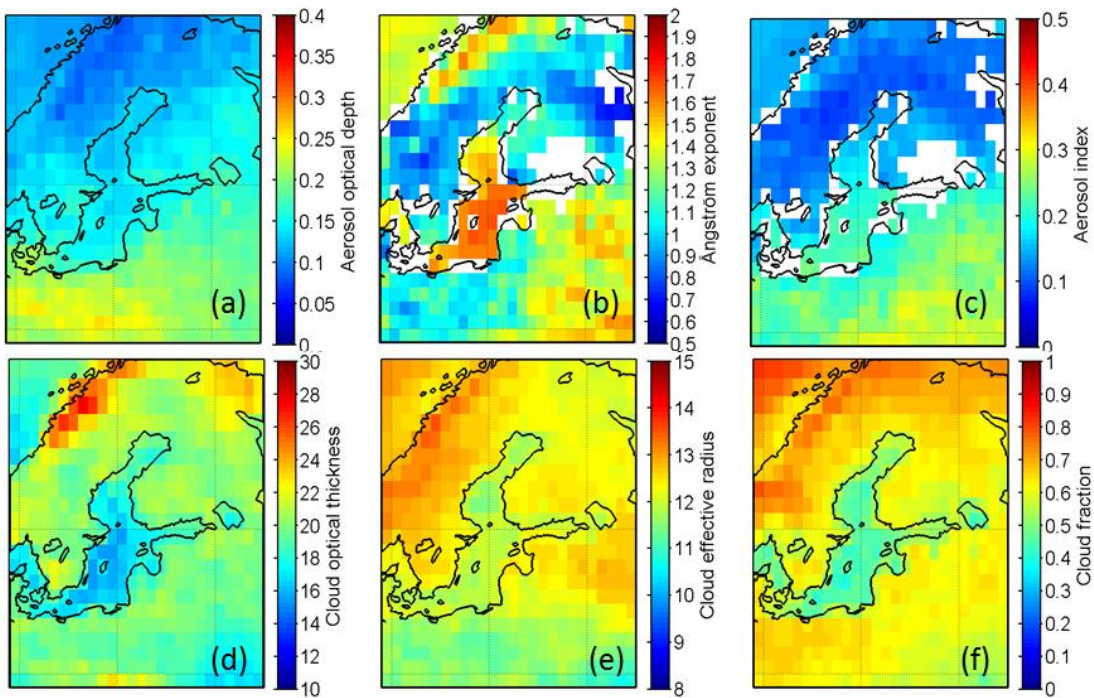
400

401 **Figure 1: The area covered in this study and its division into three sub-regions: Area 1, the Baltic Sea is represented**
 402 **by the colour Blue, Area 2, covering the land areas over Fennoscandia, is represented by colour Green and Area 3, in**
 403 **Red, includes the land areas of Central-Eastern Europe.**



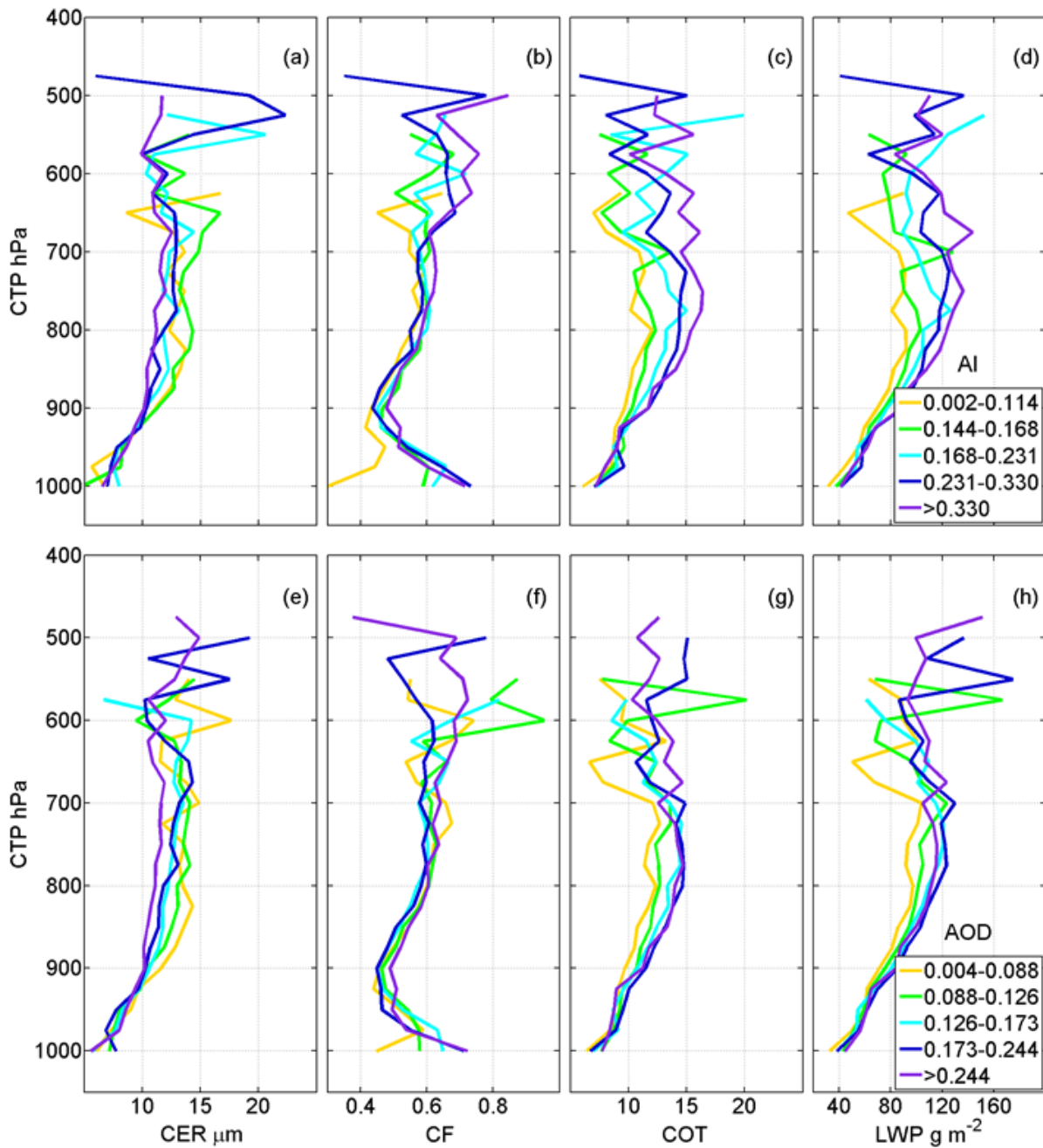
404

405 **Figure 2: Time series of summer (JJA) averages for AOD (circles) and AI (squares) for the three sub-regions. The**
 406 **three sub-regions are color-coded following that in Fig.1.**



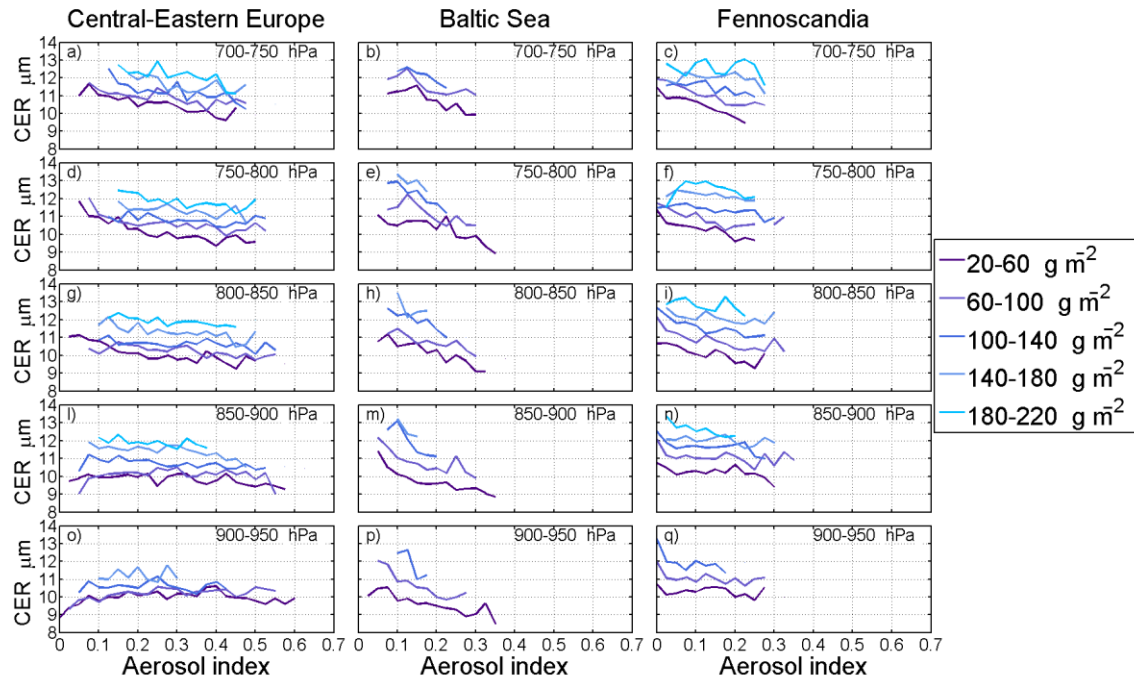
407

408 **Figure 3: Spatial distributions of AOD (a), AE (b), AI (c), COT (d), CER (e) and CF (f) averages for summer seasons**
409 **between 2003-2014.**



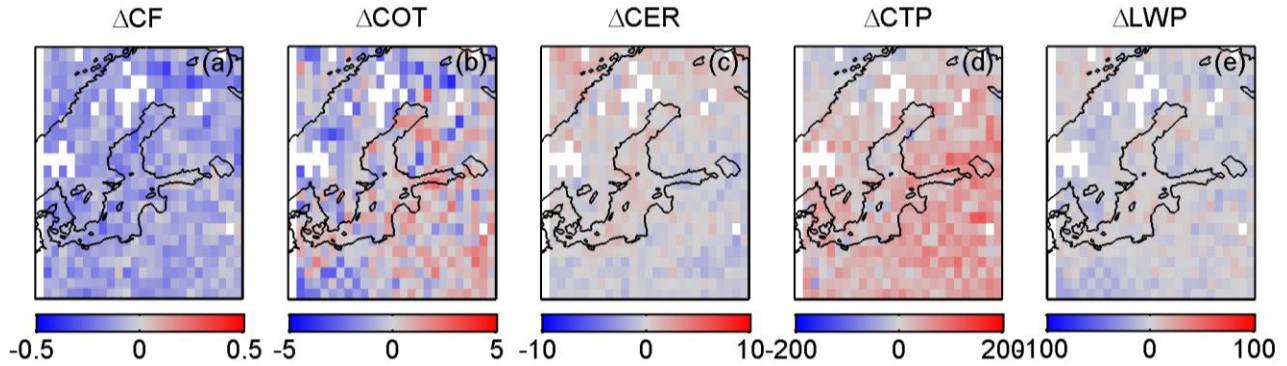
410

411 **Figure 4: 10-year averaged cloud properties as function of cloud top pressure: CER (a, e), CF (b, f), COT (c, g), LWP**
 412 **(d, h), as functions of cloud top pressure (CTP) for five classes of AI (a-d) and AOD (e-h). Each class of AI/AOD**
 413 **contains an equal number of samples in that interval.**



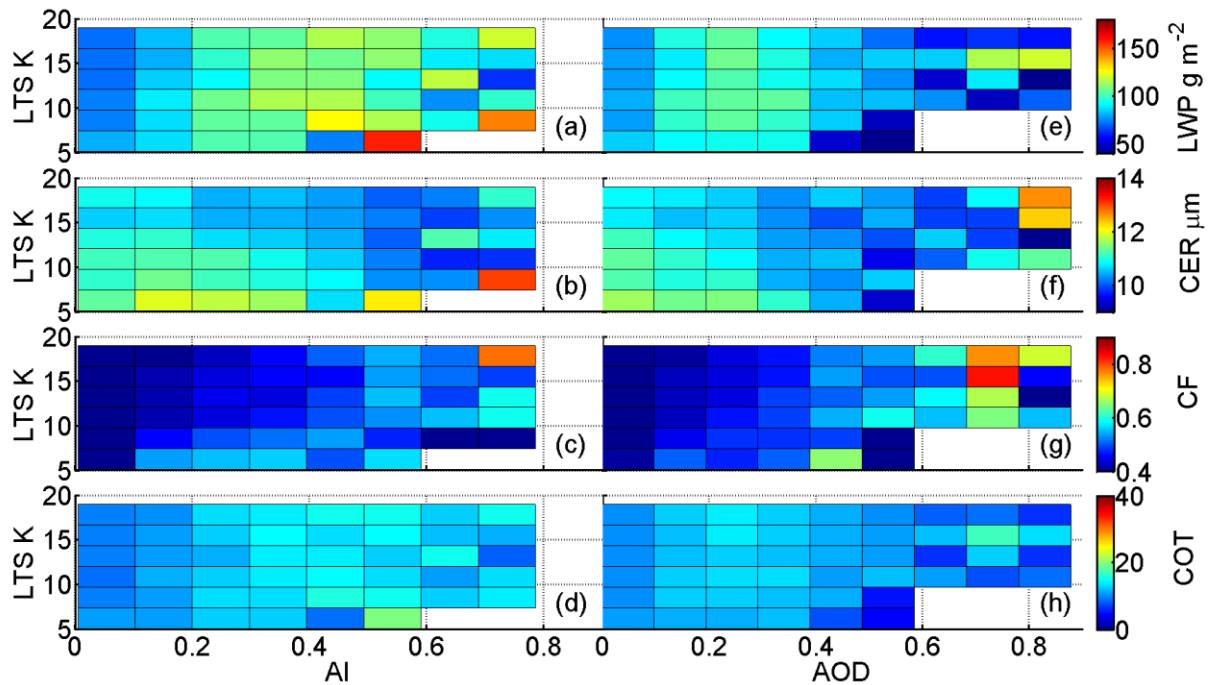
415

416 **Figure 5: CER b as function of AI, stratified for subranges of CTP and LWP, for the three sub-regions. The legend on**
 417 **the right of the figure lists the LWP bins.**



418

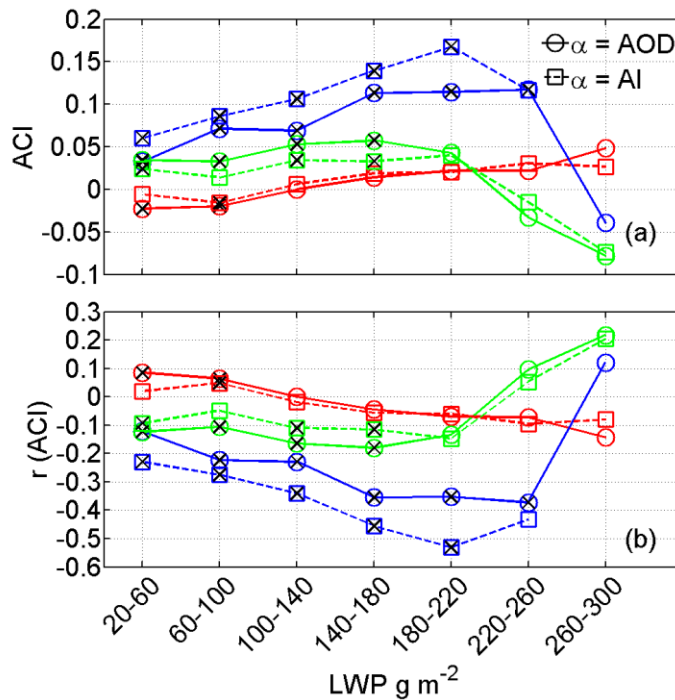
419 **Figure 6: Spatial distributions of the difference of the cloud properties CF (a), COT (b), CER (c), CTP (d), and LWP**
 420 **(e) for low aerosol loading (AOD < 25th percentile) and heavy aerosol loading (AOD > 75th percentile) calculated from**
 421 **Eq. 2.**



422

423

Figure 7: Mean low-level liquid cloud properties plotted as a function of LTS and AI (a-d) or AOD (e-h).



424

425

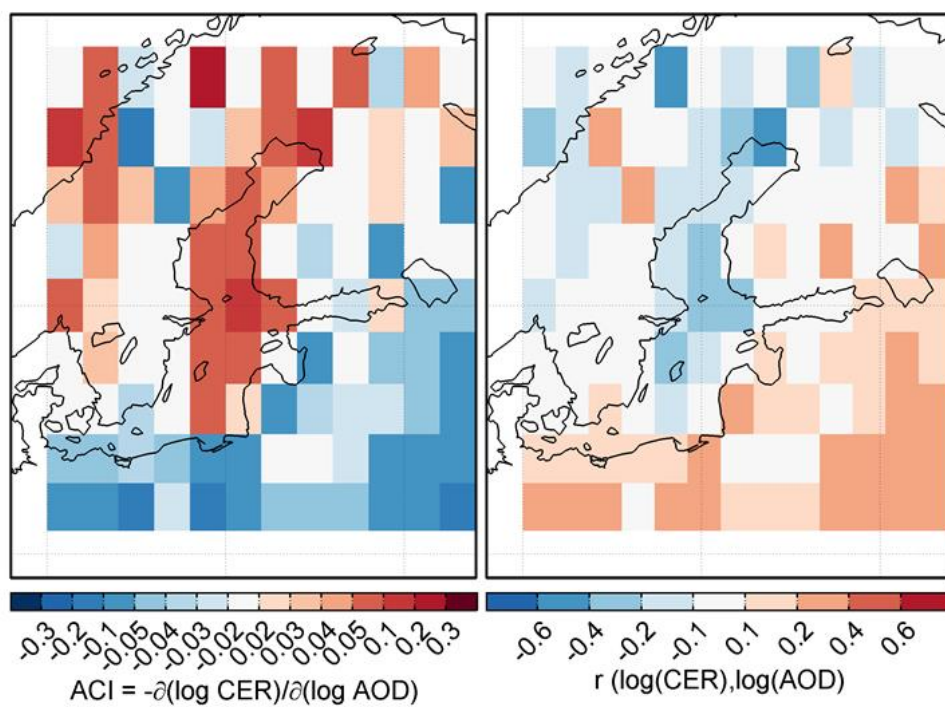
426

427

428

429

Figure 8: ACI estimates computed for the CER as a function of the LWP and by applying both the AI and AOD as proxies for the CCN are shown in (a). The correlation coefficients are presented in (b). The color-coded lines refer to the three sub-regions determined in Fig.1: Area 1 (blue), Area 2 (green) and Area 3 (red) 1. The line styles define whether the AOD or AI were used as the CCN proxy, α . Markers signed with a cross represent points fulfilling the null-hypothesis (p -value < 0.05), hence statistically significant.



430

431 **Figure 9: Applying the AOD as a proxy for the CCN, estimates of the ACI and correlation coefficient for the CER and**
 432 **for the interval of the LWP between 20-60 g/m² were calculated on a grid basis. The obtained spatial distribution of**
 433 **the ACI is shown on the left and the correlation coefficient on the right.**

434

435

436

437

438

439

440

441

442

443

444

445

446